Electronic Supplementary Information

Giuseppe Mattioli,[1, 2, *] Marcel Risch,[3] Aldo Amore Bonapasta,[1] Holger Dau,[3] and Leonardo Guidoni[4, 2, †]

[1]*Istituto di Struttura della Materia (ISM) del Consiglio Nazionale delle Ricerche,*
Via Salaria Km 29.5, CP 10, 00016 Monterotondo Stazione, Italy
[2]*Dept. of Physics, "Sapienza" Università di Roma, P.le A. Moro 2, 00185 Roma, Italy[‡]*
[3]*Dept. of Physics, Freie Universität Berlin, Arnimallee 14, 14195 Berlin, Germany*
[4]*Dipartimento di Chimica, Ingegneria Chimica e Materiali,*
Università de L'Aquila, Località Campo di Pile, 67100 L'Aquila, Italy

I.   THEORETICAL METHODS

We report here an extended description of the employed theoretical methods in order to ensure the complete reproducibility of our results. The structural and electronic properties of Co catalyst (CoCat) models have been investigated by using *ab initio* molecular dynamics (AIMD) methods[1] together with static geometry optimisations based on Density Functional Theory, as developed in the Quantum-ESPRESSO package.[2] First, the structural and electronic properties of the layered $LiCoO_2$ crystal have been investigated and compared to the available experimental data, in order to provide a reliable setup of the $Co(III)O_6$ octahedra found as basic units of the catalyst. Then, the c1, c2 and c3 Co-O clusters shown in Figure S1, containing complete and defective "cubane-like" units, have been modelled starting from the well investigated $LiCoO_2$ structure, and saturated by means of the correct number of H atoms in order to ensure a correct stoichiometry of all of the investigated systems, i.e., to enforce a +3 valence state for the Co atoms, suggested by previous XAS measurements.[3–5] Several geometry optimisation runs have been performed by accommodating the H-saturated Co-O clusters in 30 a.u.[3] cubic supercells. Total energies have been calculated by using the Γ point for the k-point sampling of the Brillouin zone, ultrasoft pseudopotentials (US),[6] and the PBE gradient corrected exchange-correlation functional.[7] Kohn-Sham orbitals have been expanded in plane waves up to energy cutoffs of 40 Ry and 320 Ry for the wavefunctions and the charge density, respectively, in order to achieve satisfactorily converged results. Such very strict convergence criteria on the plane wave basis set, as well as the inclusion of Co semicore $3s$ and $3p$ shells among the valence electrons, have proven to be necessary in order to estimate atomic distances in the most accurate way. Such values can be compared, for example, with the results provided in Ref. 8 in the case of the rutile and anatase TiO_2 polymorphs. We presented in that case an in-depth discussion of the relationship between basis set cutoff and bond distances in GGA and GGA+U calculations, applied to a different transition metal oxide investigated by using the same theoretical approach used in the case of the $LiCoO_2$ and CoCat.

In order to gain a deeper insight into the electronic properties of the CoCat, An Hubbard U correction has been applied to the system, which has been proven successful in order to improve the GGA electron correlation description in transition metal oxides and related compounds.[8–10] In detail, a Hubbard U correction for the $3d$ electrons of Co atoms was set to the average value of 7.1 eV calculated by using the self-consistent linear response approach described in Refs. 11–13 which was applied to all the nonequivalent Co atoms belonging to the c1, c2 and c3 clusters. The low spread found for the calculated U values (7.1±0.2 eV) is not expected to affect the achieved results. Moreover, in addition to this correction, an Hubbard U correction was applied to the $2p$ electrons of O atoms, because Coulomb interactions between these electrons have to be considered comparable to those between d electrons.[14–16] An U value of 5.9 eV has been estimated in this case by founding on experimental results, as suggested in Refs. 9,16. Such a twofold approach has proven to be useful to reproduce the strong $p - d$ coupling reported on the ground of PES investigations in Ref. 17 in the case of the $LiCoO_2$ crystal (see Figure S3).

Ab initio molecular dynamics (AIMD) simulations[1,2], based on a similar theoretical approach, were performed at the GGA level to investigate finite temperature properties of selected clusters, both in gas phase and in solution. Such calculations have been carried out by using a 0.073 fs (3 a.u.) time step and a 300 K temperature controlled by Nose thermostats for about 10-12 ps. In the case of solvated simulations, the c2 cluster have been surrounded by 58 water molecules which have been placed and relaxed by using the "point and click" Avogadro[20] tool. Then, a Nose-Parrinello-Rahman NPT simulation was performed until the internal pressure reached negligible values and the cubic simulation cell shrunk from the value of 30 a.u.[3] to an average value of 24.4 a.u.[3]. A complete summary of the achieved results is displayed in Table SI.
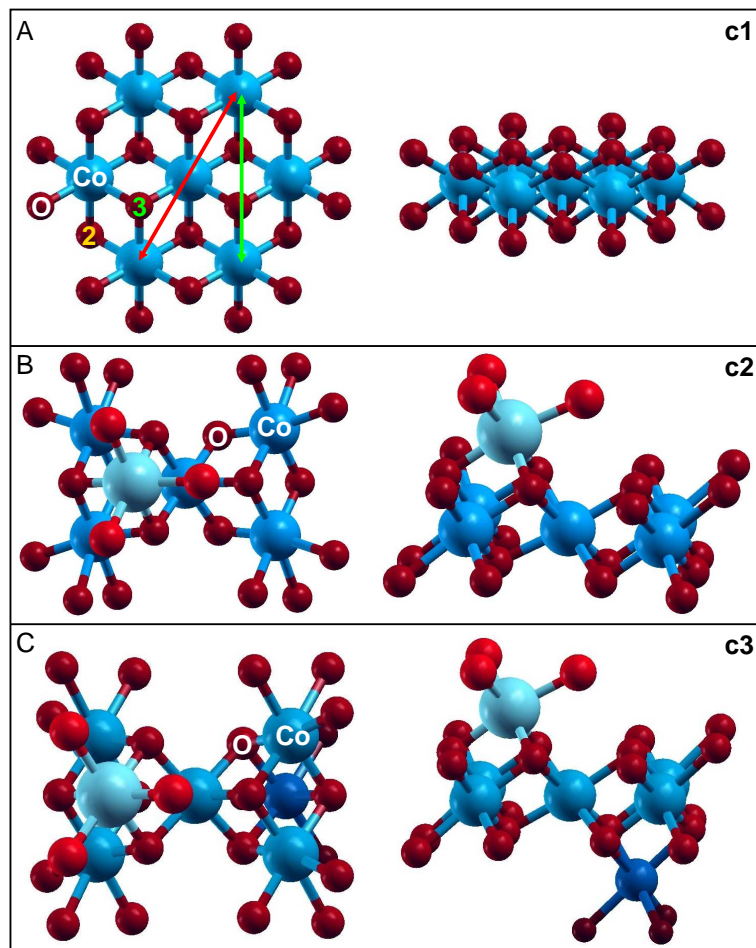
FIG. S1: Top and side view of: (A) Co_7O_{24} c1 cluster; (B) Co_6O_{23} c2 cluster; (C) Co_7O_{26} c3 cluster. Larger spheres and brighter colours indicate atoms belonging to topmost layers. "2" and "3" labels indicate examples of μ_2-O and μ_3-O sites. The red and green lines in the upper panel identify three collinearly arranged Co atoms (Co-Co 3 distance in Table SI) and 2 Co atoms separated by oxo bridges (Co-Co 2 distance in Table SI), respectively.

II. LICOO$_2$ RESULTS

To assess the capability of our *ab initio* calculation to predict Co-O and Co-Co distance at sufficient precision, we have investigated a crystallographically (XRD) characterized Co-oxo compound with close structural similarity to the CoCat, namely $LiCoO_2$. This material consists of Co-O sheets of interconnected defective cubane units (layers of edge-sharing $Co(III)O_6$ octahedra) separated by intercalated Li^+ ions (Figure S3). In detail, we validated our theoretical setting by performing simulations of the $LiCoO_2$ properties by using a 12-atom hexagonal unit cells and a 24-atom tetragonal supercell, the latter being used in order to avoid spurious results due to spin-frustration phenomena in a unit cell containing an even number of Co atoms. Satisfactorily converged results were achieved by using a $8 \times 8 \times 4$ **k**-point mesh for both the cells, and the above mentioned 40/320 Ry cutoffs. Concerning the structural properties of the $LiCoO_2$, we have estimated lattice parameters values at the GGA level (a=2.854 Å and c=14.025 Å) in close agreement with experimental ones (a=2.816 Å and c=14.044 Å).[21] An even closer agreement have been achieved in the case of GGA+U results (a=2.828 Å and c=14.114 Å). A further set of simulations have been carried out by using norm-conserving Martins-Troullier pseudopotentials[22] and 140/560 Ry cutoffs in order to show that the achieved results are not biased by the choice of a particular kind of pseudopotential. Table SI provides a comparison of distances obtained experimentally (by XRD[19] and XAS[18] measurements) and calculated by different *ab initio* approaches. Experimentally determined and calculated distances agree reassuringly well. Using the GGA+U approach, the deviations are around 0.02 Å; slightly more pronounced deviations were observed in the GGA simulation. In conclusion, both the XAS and *ab initio* calculations have passed the $LiCoO_2$ test. Both methods have reproduced sufficiently well the atom-atom distances of the first (Co-O) and second (Co-Co) coordination spheres
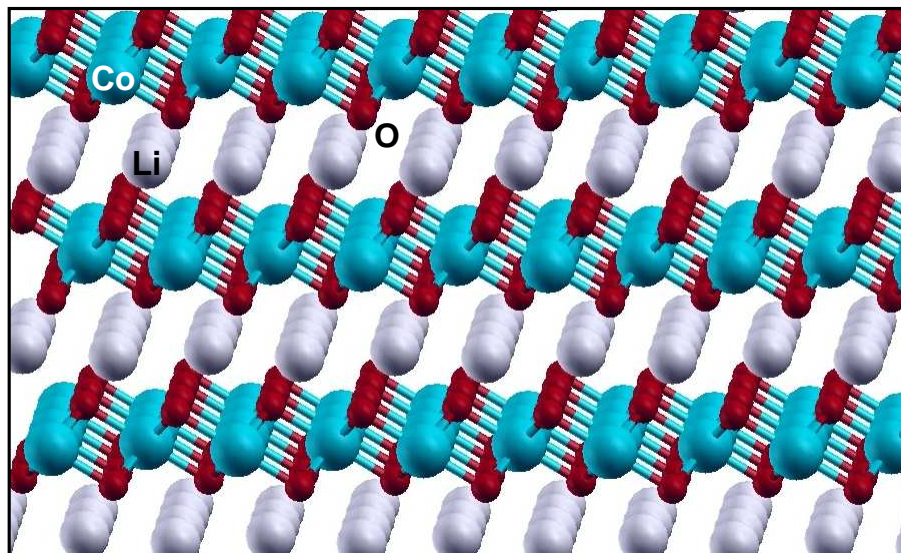
FIG. S2: Structure of the layered $LiCoO_2$ bulk crystal. Layers of Li atoms are intercalated between CoO_2 layers formed by $Co(III)O_6$ octahedra.

On the side of the electronic properties, the GGA approach underestimates the Kohn-Sham energy gap: a value of 1.5 eV has to be compared to the experimental value of 2.7 eV.[17] Moreover, the strong hybridisation between O $2p$ and Co $3d$ orbitals, reported on the ground of photoemission electron spectroscopy measurements,[17] is only slightly appreciable at a GGA level, as shown by the projected Density Of States (pDOS) in Figure S3 A. Both these issues result to be improved in the case of GGA+U calculations: a strong O $2p$ - Co $3d$ mixing is clearly shown by the pDOS in figure S3 B and a (slightly overestimated) energy gap value of 3.3 eV has been calculated within a GGA+U approach.

III. XAS ANALYSIS

We are aiming at a comparison of characteristic inter-atomic distances obtained by *ab initio* calculations and by XAS measurements at the K-edge of cobalt. In XAS, the primary structural tool is analysis of the extended X-ray absorption fine-structure (EXAFS), that is, the oscillatory fine-structure in a spectral region extending up to 1000 eV above the absorption threshold.[23–25] In our work, determination of absorber-backscatterer distances is approached by spectral simulation of the k^3-weighted EXAFS spectrum, $k^3\chi(k)$, with k being the wavenumber of the photoelectron. By EXAFS simulations, the distances between the X-ray absorbing Co ion and the backscattering atoms of the first (O, 1.9 Å) and second coordination sphere (Co, 2.8 Å) can be determined at a precision that may exceed 0.02 Å. This high precision is obtained for the mean distance of an atom shell with a roughly Gaussian shaped distance distribution function, with a width described by the EXAFS Debye-Waller factor (σ).[23–25] For $LiCoO_2$, we find that the mean distances ('Co-O' and 'Co-Co 1' in Table SI) determined by XAS and XRD differ by only 0.01 Å, thereby confirming the accuracy of the used EXAFS analysis approach. (It is important to note that mostly the σ-value is clearly greater than the imprecision in the respective mean distance.)

In order to provide experimental evidence for the occurrence of protonated μ_2-O sites in the CoCat samples, a new, more appropriate analysis of previous XAS measurements[3] has been performed together with further, ancillary GGA calculations. Such calculations have regarded the gas-phase c2 cluster with different configurations of the saturating H atoms. Different (locally stable) equilibrium geometries have been found where some non protonated μ_2-O bridges occur. An average Co-Co nearest-neighbour distance of 2.76 Å has been extracted by such structures, which represents a sizeably different estimate with respect to the 2.81 Å average value found in the case of Co-Co 1 distances (see Table SI for comparison). Subsequently, we devised a refined simulation approach tailored to test if an abundance of these 2.76 Å distances is compatible with the previously reported XAS data.[3] The Co-Co distances which correspond to protonated (2.81 Å) and unprotonated (2.76 Å) μ-oxo bridges were fixed to eliminate the high correlation between such closely situated shells. Moreover, the core of our hypothesis is the abundance of exactly these two distances which in itself justifies the fixation of simulation parameters. The Debye-Waller parameter (σ) of the shorter Co-Co distance was also fixed to prevent further parameter correlation and to ensure the same number of free parameters than in the

TABLE SI: **Upper Table:** structural properties of the most stable gas phase c1, c2 and c3 clusters, shown in Figure S1 as well as of the LiCoO$_2$ crystal. Static (GGA, GGA with norm conserving pseudopotentials (NC), and GGA+U) and AIMD results have been displayed for comparison. The Co-O (inner) column is related only to Co-O bonds belonging to the cubane structures, whereas the Co-O (all) column is related to all the Co-O bonds. We have taken into account distances related only to O atoms interconnecting Co atoms because such distances do not depend upon the presence of different species at the cluster boundaries (counterions like PO$_4^{3-}$ as well as further cubane units not included in present simulations) and are more likely to represent Co-O bonds in the catalyst structure. The Co-Co 1 label denotes the distance between Co-Co nearest neighbours separated by a μ-oxo bridge; Co-Co 2 is the shortest distance between two Co atoms which are not directly connected by a μ-oxo bridge, and Co-Co 3 is the distance between the far atoms in three collinearly arranged Co atoms. **Lower Table:** structural properties of the stablest solvated c2 cluster, (see Figure 2 in the main text). The Co-O (inner) column is related to all the Co-O bonds belonging to the cubane structures. The Co-O (μ_3) column is related to Co-O bonds involving μ_3-O atoms. The Co-O (μ_2) column is related to Co-O bonds involving μ_2-O atoms. Co-Co 1, 2 and 3 columns are analogous with the upper table ones. The (com) and (def) labels indicate Co-Co nearest neighbour distances within the complete and the defective cubane structures, respectively. In the case of static GGA and GGA+U simulations, data have been averaged on different bonds of the same type, whereas they have been averaged on different bonds of the same type and along the trajectory in the case of 10 ps AIMD simulations at 300 K (12 ps at 300 K in the case of the c2+58H$_2$O (AIMD)). The values in parentheses for the XAS data corresponds to the Debye-Waller parameter (σ) as obtained by EXAFS simulations; Further details on XAS data can be found in Refs. 3,18. LiCoO$_2$ XRD data are taken from Ref. 19

Structure (Method)	Bond Distance (Å) [Coordination Number of Co Atoms]				
	Co-O (all)	Co-O (inner)	Co-Co 1	Co-Co 2	Co-Co 3
c1 (GGA)	1.94±0.08 [6.0]	1.91±0.05	2.79±0.02 [3.4]	4.84±0.02 [1.7]	5.59±0.02 [0.9]
c1 (GGA+U)	1.93±0.07 [6.0]	1.90±0.05	2.80±0.02 [3.4]	4.85±0.02 [1.7]	5.60±0.02 [0.9]
c1 (AIMD)	-	1.91±0.05	2.81±0.06	4.86±0.07	5.61±0.07
c2 (GGA)	1.94±0.06 [6.0]	1.90±0.03	2.80±0.04 [3.0]	4.73±0.14 [1.3]	5.56-5.61 [0.7]
c2 (GGA+U)	1.93±0.06 [6.0]	1.89±0.03	2.80±0.04 [3.0]	4.70±0.16 [1.3]	5.56-5.61 [0.7]
c2 (AIMD)	-	1.90±0.07	2.81±0.08	4.85±0.20	5.63±0.11
c3 (GGA)	1.95±0.09 [6.0]	1.88±0.03	2.79±0.03 [3.4]	4.81±0.06 [1.7]	5.56±0.01 [0.9]
c3 (GGA+U)	1.94±0.09 [6.0]	1.88±0.03	2.78±0.02 [3.4]	4.79±0.07 [1.7]	5.54±0.01 [0.9]
c3 (AIMD)	-	1.89±0.06	2.79±0.06	4.82±0.11	5.56±0.08
CoCat XAS data	1.89(0.05) [5.8]	-	2.81(0.07) [3.7]	4.86 [0.5-0.7]	5.62(0.07) [0.9]
LiCoO$_2$ (GGA)	1.936	-	2.854	4.944	5.709
LiCoO$_2$ (GGA NC)	1.935	-	2.840	4.919	5.680
LiCoO$_2$ (GGA+U)	1.926	-	2.828	4.898	5.656
LiCoO$_2$ XAS data	1.91(0.06)		2.81(0.05)	4.94(0.05)	5.61(0.03)
LiCoO$_2$ XRD data	1.92(5)	-	2.816(6)	4.878(5)	5.633(2)

Structure (Method)	Bond Distance (Å)							
	Co-O (inner)	Co-O (μ_3)	Co-O (μ_2)	Co-Co 1	Co-Co 1 (com)	Co-Co 1 (def)	Co-Co 2	Co-Co 3
c2 (AIMD)	1.90±0.07	1.88±0.05	1.97±0.06	2.81±0.08	2.79±0.07	2.86±0.07	4.85±0.20	5.63±0.11
c2+58H$_2$O (AIMD)	1.91±0.05	1.90±0.05	1.95±0.06	2.84±0.06	2.83±0.06	2.86±0.06	4.77±0.16	5.65±0.08
c2+58H$_2$O (GGA)	1.91±0.03	1.89±0.03	1.97±0.02	2.83±0.02	2.83±0.02	2.83±0.03	4.75±0.13	5.59-5.64
c2+58H$_2$O (GGA+U)	1.91±0.02	1.89±0.03	1.96±0.02	2.84±0.03	2.83±0.03	2.84±0.02	4.75±0.17	5.60-5.66
CoCat XAS data	1.89(0.05)	-	-	2.81(0.07)	-	-	4.86	5.62(0.07)

previous evaluation,[3] thus enabling a direct comparison between the two approaches. We found that the constraint of the Debye-Waller parameter did not have a strong influence on the result of the hypothesis test, see Figure S5 and the corresponding discussion below. In addition to the Debye-Waller parameter, the number of Co neighbours was also fixed in order to act as the independent variable of our hypothesis test. All other parameters of the EXAFS simulation, in particular the first shell (Co-O bond) were allowed to vary freely, thus ensuring enough degrees of freedom for proper
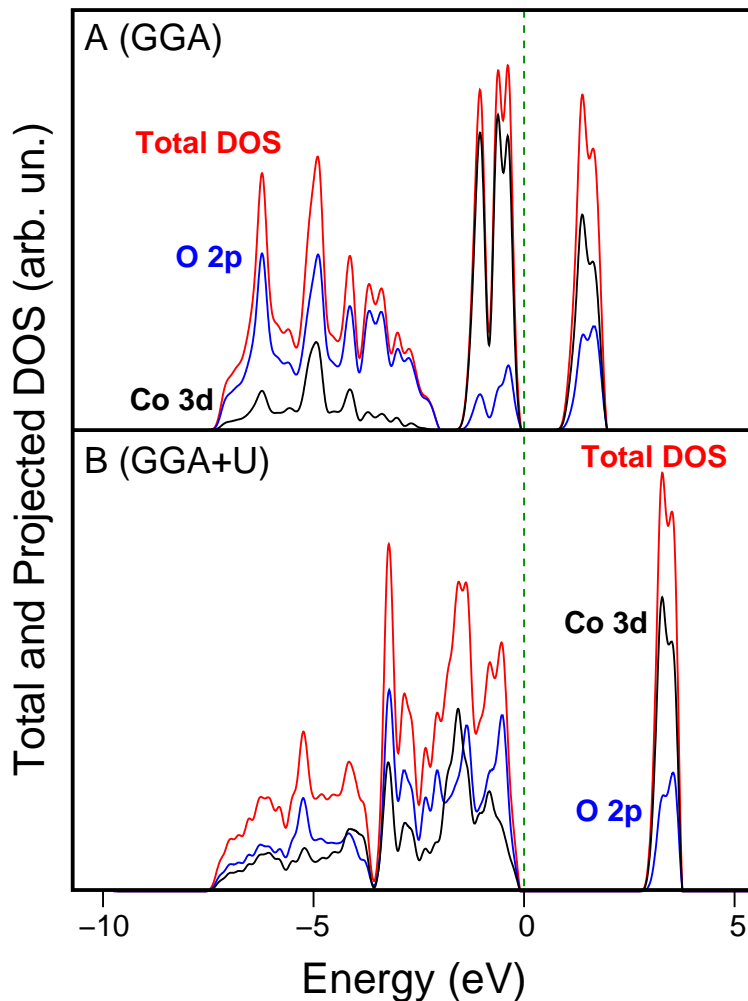
FIG. S3: Total (red lines) and Projected on O $2p$ (blue lines) and Co $3d$ (black lines) atomic orbitals DOS (density of states) of the layered $LiCoO_2$ bulk crystal. Panel A: GGA case; Panel B: GGA+U case. A zero energy value has been assigned to the valence band maximum in both cases.

TABLE SII: Parameters of the EXAFS simulations shown in Figure S4. The parameters marked by a star ($\star$) were fixed, and all other parameters were determined by curve-fitting of the data (k range 3-12 Å^{-1}). The EXAFS coordination, N, represents the number of backscattering atoms per absorbing cobalt at a distance close to R. σ denotes the Debye-Waller parameter. $M(x)$ is the result of χ^2 minimization (see equation 1) and Rf, defined in Ref. 3, is the quality of fit (distances between 2.1 and 2.9 in the reduced scale were used in the calculation). For both variables, a lower value indicates a better agreement between simulation and experimental data.

	Co-O			Co-Co 1 (2.81 Å)			Co-Co 1 (2.76 Å)				
Short Dist. %	N	R (Å)	σ (Å)	N	R (Å)	σ (Å)	N	R (Å)	σ (Å)	$M(x)$	Rf
0.00	5.77	1.891	0.052	4.01	2.81*	0.068	0.00*	2.76*	0.05*	18.0	8.6
20.27	5.89	1.892	0.054	3.07	2.81*	0.064	0.78*	2.76*	0.05*	30.0	17.9
40.55	6.00	1.892	0.057	2.20	2.81*	0.058	1.50*	2.76*	0.05*	63.4	31.3
60.32	6.09	1.892	0.059	1.41	2.81*	0.047	2.15*	2.76*	0.05*	111.9	43.6

minimization of the χ^2 function used in EXAFS simulations (equation 1). The minimization results of the refined simulation approach have been collected in Table SII. A graphical representation of the solutions is given in Figure S4. Both renderings are presented as a function of the fraction of unprotonated Co-Co bonds which is given under
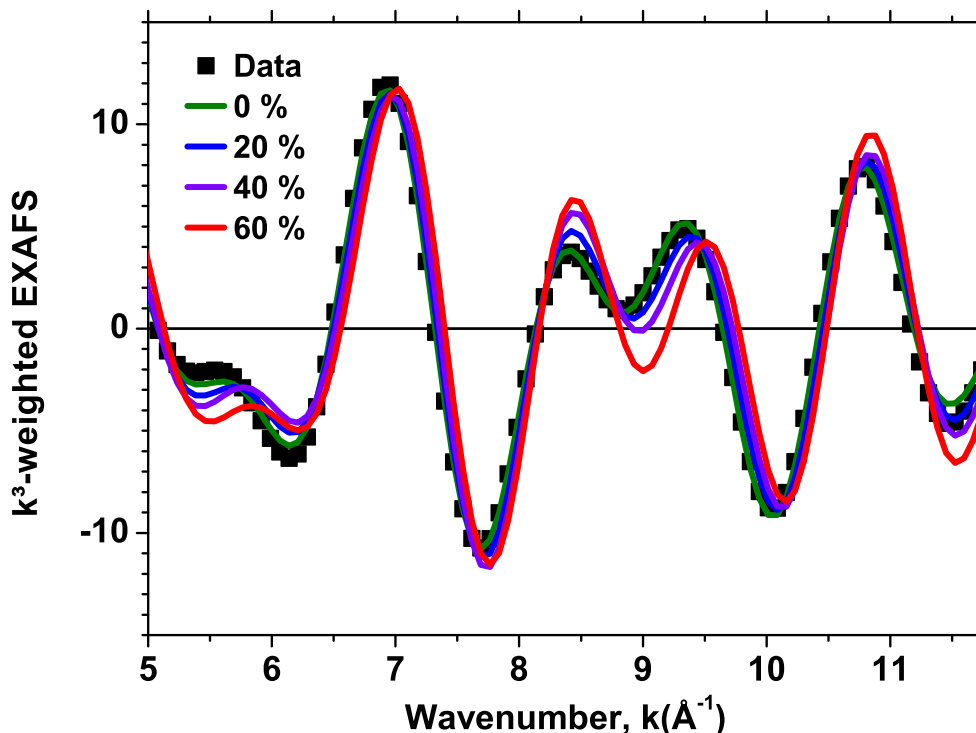
FIG. S4: Measured and simulated EXAFS (Extended X-ray absorption Fine-Structure) spectra for various contributions of Co-Co distances of 2.76 Å length. The EXAFS of the CoCat was measured and processed as described elsewhere.[3] The EXAFS data was simulated assuming various fractions (0%, 20%, 40%, and 60%) of Co-Co vectors of 2.76 Å length, which is the likely Co-Co distance for a Co-(μ_2-O)(μ_3-O)-Co motif. These simulations suggest that a contribution of short Co-Co distance of 20% or more would be incompatible with the experimental results. The coordination number of the 2.81 Å vector was a free fit parameter. Both data and simulation were Fourier-filtered between 1.2 and 2.8 Å (reduced scale) after simulation in k-space for clarity of the presentation. We emphasize that the simulations were performed on unfiltered data. The refined simulation approach is discussed in section III.

the assumption that the total number of Co-Co vectors at 2.76 Å and 2.81 Å equals 100%. The simulation deviates significantly from the measured XAS data for any appreciable contribution of 2.76 Å distances, which can be seen clearly and intuitively in Figure S4 and also in Table SII where M(x), the result of the χ^2 minimization (an rms error) strongly increases with the amount of short distances.

The statistical significance of these results was tested in order to evaluate the initial hypothesis. The results are based on the following definition of the χ^2 function

$$\chi^2 = \frac{N_{ind}}{pts} \sum_1^{pts} k^{2w} \frac{(data - model)^2}{E^2} \tag{1}$$

with $N_{ind} = \frac{2\Delta r \Delta k}{\pi} + 1$ as the number of statistically independent points, pts as the number of data points in the file, k^{2w} as the k-space weighting factor, E^2 as the normalization factor to yield the proper expectation value (i.e. the degrees of freedom in the simulation). We used a scaling factor of $E^2 = 0.73$ to ensure that the χ^2 function was normalized to 18 degrees of freedom. The minima of the χ^2 function lie on a parabola given by

$$M(x) = M(a) + \frac{(x - a)^2}{\sigma_a^2} \tag{2}$$

where $M(a)$ denotes the global minimum of parameter space which occurred for 0% short distances (see Table SII). Equation 2 has the property

$$M(a \pm n\sigma_a) = M(a) + n^2 \tag{3}$$

(a) Debye-Waller parameter of 0.03 Å   (b) Debye-Waller parameter of 0.05 Å   (c) Debye-Waller parameter of 0.07 Å
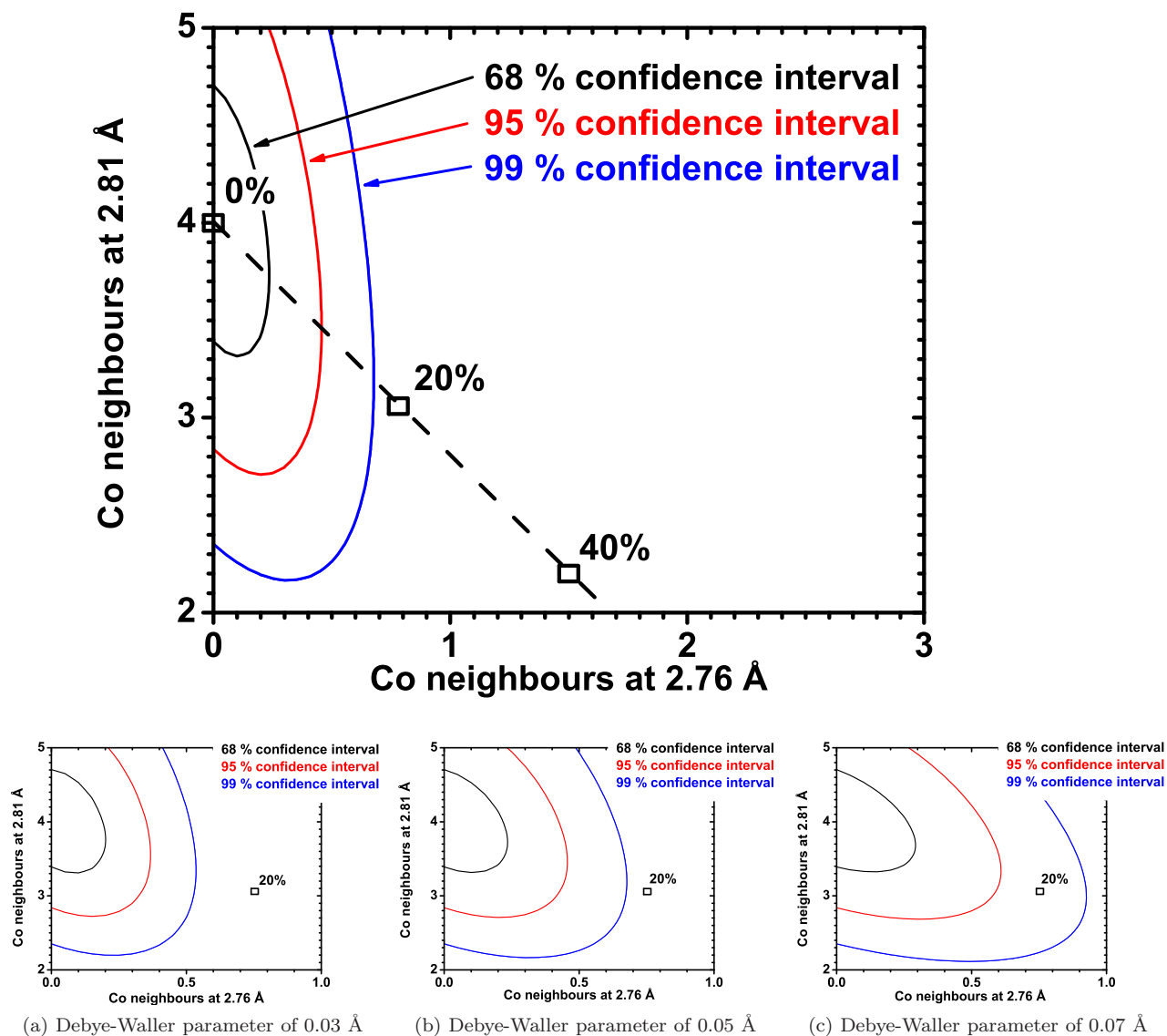
FIG. S5: **Upper Panel:** Contour plot of the minimization error of 6161 EXAFS simulations. The number of Co neighbours for both shells were fixed to the values on the axis. The same parameters than for the simulation shown in Table SII were fixed. The open squares represent the simulation results shown in Figure S4. It can be seen clearly that 20% contribution of short distances is incompatible with the experimental data within 99% confidence interval. The dashed line is guide to the eye along which the solutions shown in Figure S4 lie. **Lower Panels:** Variation of the confidence ellipsoids with the variation for the Debye-Waller parameter of the Co shell at 2.76 .

Therefore, the 68%, 95%, 99% confidence intervals are given by $M(a) + 1$, $M(a) + 4$, $M(a) + 9$, respectively.[26] In order to capture non-linear effects of the confidence ellipsoids (χ^2 mimization of the EXAFS function is a highly non-linear problem), we evaluated 6161 individual EXAFS simulations in which the number of Co-Co neighbours at the protonated (2.81 Å) and non-protonated (2.76 Å) sites was fixed to the values shown on the axes in Figure S5 (upper panel). The same constraints than for the previous simulations (cf. Table SII) were used, i.e. many parameters ran freely. The high number of EXAFS simulations was imposed by the requirement for good resolution in both variables which is necessary for the calculation of the fraction of short distances. In order to test the influence of the fixed Debye-Waller parameter in the shell with short Co-Co distances, we repeated the above procedure with physically reasonable lower and higher boundaries for the Debye-Waller parameter. In any physically reasonable system, the hypothesis of an abundance of short distances (arbitrarily defined by the 20% mark) can be rejected within at least the 95% confidence interval. For a Debye-Waller parameter of 0.05 Å and lower, an abundance of the unprotonated

shorter mean distances is incompatible with the experimental data within 99% confidence interval. It is expected that the value of the Debye-Waller parameter is somewhat lower than the value of 0.07 Å reported in[3] because splitting of one shell into two shells with close distance modes (for Gaussian distributions also the mean distances) should reduce the distance standard deviation of both new shells. Qualitatively, this behavior is observed for the shell at 2.81 with increasing contribution of shorter distances.

---

[*] Electronic address: giuseppe.mattioli@ism.cnr.it

[†] Electronic address: leonardo.guidoni@univaq.it

[‡] Current address: Dept. of Chemistry, "Sapienza" Università di Roma, P.le A. Moro 2, 00185 Roma, Italy

[1] R. Car and M. Parrinello, *Phys. Rev. Lett.*, 1985, **55**, 2471–2474.

[2] P. Giannozzi et al., *J. Phys.: Condens. Matter*, 2009, **21**, 395502.

[3] M. Risch, V. Khare, I. Zaharieva, L. Gerencser, P. Chernev and H. Dau, *J. Am. Chem. Soc.*, 2009, **131**, 6936.

[4] M. W. Kanan, J. Yano, Y. Surendranath, M. Dinca, V. K. Yachandra and D. G. Nocera, *J. Am. Chem. Soc.*, 2010, **132**, 13692.

[5] H. Dau, C. Limberg, T. Reier, M. Risch, S. Roggan and P. Strasser, *ChemCatChem*, 2010, **2**, 724.

[6] D. Vanderbilt, *Phys. Rev. B*, 1990, **41**, 7892–7895.

[7] J. P. Perdew, K. Burke and M. Ernzerhof, *Phys. Rev. Lett.*, 1996, **77**, 3865–3868.

[8] G. Mattioli, F. Filippone, P. Alippi, R. Caminiti and A. Amore Bonapasta, *J. Phys. Chem. C*, 2010, **114**, 21694.

[9] C. Cao, S. Hill and H.-P. Cheng, *Phys. Rev. Lett.*, 2008, **100**, 167206.

[10] H. Hsu, K. Umemoto, M. Cococcioni, and R. Wentzcovitch, *Phys. Rev. B*, 2009, **79**, 125124.

[11] M. Cococcioni and S. de Gironcoli, *Phys. Rev. B*, 2005, **71**, 035105.

[12] H. J. Kulik, M. Cococcioni, D. A. Scherlis and N. Marzari, *Phys. Rev. Lett.*, 2006, **97**, 103001.

[13] D. A. Scherlis, M. Cococcioni, P. Sit and N. Marzari, *J. Phys. Chem. B*, 2007, **111**, 7384–7391.

[14] M. R. Norman and A. J. Freeman, *Phys. Rev. B*, 1986, **33**, 8896.

[15] A. K. McMahan, R. M. Martin and S. Satpathy, *Phys. Rev. B*, 1988, **38**, 6650.

[16] I. A. Nekrasov, M. A. Korotin and V. I. Anisimov, *V. I. Anisimov*, 2008, arXiv:cond-mat/0009107v1.

[17] V. R. Galakhov, E. Z. Kurmaev, S. Uhlenbrock, M. Neumann, D. G. Kellerman and V. S. Gorshkov, *Solid State Comm.*, 1996, **99**, 221.

[18] M. Risch, F. Ringleb, V. Khare, P. Chernev, I. Zaharieva and H. Dau, *J. Phys.: Conf. Series*, 2009, **190**, 012167.

[19] W. D. Johnston, R. R. Heikes and D. Sestrich, *J. Phys. Chem. Solids*, 1958, **7**, 1.

[20] http://avogadro.openmolecules.net/wiki/Main_Page.

[21] Y. Shao-Horn, S. A. Hackney, A. J. Kahaian and M. M. Thackeray, *J. Solid State Chem.*, 2002, **168**, 60.

[22] N. Troullier and J. L. Martins, *Phys. Rev. B*, 1991, **43**, 1993.

[23] B. Teo, *EXAFS: Basic Principles and Data Analysis*, Springer Verlag, Berlin, Germany, 1986.

[24] G. N. George, B. Hedman and K. O. Hodgson, *Nat. Struct. Biol.*, 1998, **5**, 645.

[25] H. Dau, P. Liebisch and M. Haumann, *Anal. Bioanal. Chem.*, 2003, **376**, 562.

[26] W. T. Eadie, D. Drijard, F. James, M. Roos and B. Sadoulet, *Statistical Methods in Experimental Physics*, North-Holland, 1971.